SCIENCE CHINA
Information Sciences

• RESEARCH PAPER •

November 2024, Vol. 67, Iss. 11, 212303:1–212303:12
https://doi.org/10.1007/s11432-024-4151-8

Securing STAR-FC-RIS empowered integrated sensing and multiuser communications against target eavesdropping

Shuying LIN[1], Yulong ZOU[1*], Fu XIAO[2] & Bin LI[3]

[1]*School of Telecommunications and Information Engineering, Nanjing University of Posts and Telecommunications, Nanjing* 210003*, China;*
[2]*School of Computer Science, Nanjing University of Posts and Telecommunications, Nanjing* 210023*, China;*
[3]*Key Laboratory of Broadband Wireless Communication and Sensor Network Technology, Nanjing University of Posts and Telecommunications, Nanjing* 210003*, China*

Received 15 June 2024/Revised 2 September 2024/Accepted 12 September 2024/Published online 23 October 2024

Abstract This paper investigates a simultaneous-transmitting-and-reflecting fully-connected reconfigurable intelligent surface (STAR-FC-RIS) empowered integrated sensing and multiuser communications (ISAMC) network, where a dual-functional radar-communication base station detects a malicious radar target nearby and communicates with multiple legitimate users on the other side of the STAR-RIS. We utilize an integrated architecture that combines the fully-connected (FC)-RIS, an emerging type of beyond-diagonal (BD)-RIS, with the time-switching (TS)-STAR-RIS to enhance both the sensing and communications at the cost of possible target intercepting and propose the simultaneous-transmitting-and-reflecting fully-connected RIS (STAR-FCR) schemes to strike a balance between sensing and communications performance. Thereafter, observing the security-reliability performance tradeoff of the downlink ISAMC, we conduct closed-form analyses to compare COPs of round-robin scheduling (RS) and multiuser scheduling (MS) with the aid of a TS-based STAR-FC-RIS. Furthermore, we derive closed-form expressions of the sensing outage probability, communications outage probability (COP), and communications intercept probability, where an average of the three probabilities is exploited to obtain an optimized time allocation (OTA) of the STAR-FC-RIS. Numerical results verify that the STAR-FCR-MS scheme outperforms the STAR-FCR-RS scheme in terms of sensing reliability and communications security. Moreover, an OTA remarkably enhances the overall performance of the STAR-FCR schemes of ISAMC systems.

Keywords simultaneous-transmitting-and-reflecting reconfigurable intelligent surface (RIS), fully-connected beyond-diagonal RIS, integrated sensing and communications, multiuser scheduling, security

1 Introduction

The flourishing Internet of Things (IoT) technology is enabling the ubiquitous connectivity of intelligent devices from smart mobile phones to driverless vehicles. The applications require billions of sensors with multiple integrated wireless functionalities, such as high-quality communications and high-accuracy sensing [1]. To this end, integrated sensing and communication (ISAC) has been regarded as a promising paradigm [2, 3]. Generally, in ISAC systems, the combination of sensing and communications is developed at different levels. At an earlier stage, only the overlapped frequency bands were considered for the co-existence of radar and communication systems, where the coordination gain of two functions requires prohibitive feedback overhead to exchange information [4,5]. Until recently, the shared hardware architectures over the same time-frequency resources in ISAC systems have come on the scene with a well-designed unified dual-function radar communication (DFRC) signal. The common signal highlights an existence of the performance tradeoff between sensing and communications due to mutual interferences between the two functionalities [6].

Despite the potential of ISAC systems to alleviate spectrum scarcity issues caused by increasing data rates, their performance gains are extremely limited due to uncontrollable electromagnetic environments

* Corresponding author (email: yulong.zou@njupt.edu.cn)

in practical settings [7]. As a remedy, by virtue of the unprecedented capability of reconfiguring the radio environment [7,8], reconfigurable intelligent surfaces (RISs) have been proposed as an appealing solution in ISAC systems [9–12]. Previous studies have explored the use of RISs in ISAC systems, such as a two-stage transmission protocol for RIS-aided ISAC systems proposed in [8], taking advantage of two sub-surfaces and the pre-knowledge of user location information obtained by sensing. Nevertheless, the described RIS-aided ISAC systems raise tremendous security concerns [11,12]. On the one hand, the shared wireless environment of extra links established by an enormous number of RIS elements makes confidential information vulnerable to potential eavesdropper attacks. On the other hand, for a secure wireless system, it is undesirable for the communication information in DFRC waveforms to reach an untrusted target, i.e., a potential eavesdropper. Furthermore, a joint transmitting and reflecting RIS should even be more carefully designed considering the physical layer security problem [13]. In RIS-aided ISAC systems, the conventional performance indicators for secure communications without target detection can be extensively used [14]. For instance, an outage event usually refers to the case that the instantaneous transmission rate falls below a target threshold, whose occurrence probability is named outage probability (OP). Also, intercept probability (IP) is defined as the probability that the eavesdropping rate is higher than the difference between the data rate and the required secrecy rate. Notably, the OP has been regarded as a performance indicator for evaluating reliability in various studies. Furthermore, the security-reliability tradeoff (SRT) performance is exhibited by an OP expression with regard to its corresponding IP, which results in a decreasing function [15]. This is because although higher transmit power improves the transmission reliability in terms of a decreasing OP, it also brings about a strengthened signal received at an eavesdropper which does harm to secrecy performance. In ISAC systems, the target detection usually relies on the sensing signal echoed from the target. So the sensing outage happens when the probing channels and echo channels degrade, but is independent of communications links. It is worth mentioning that in other works on wireless security [16], the detection can also refer to receiving confidential messages, which is an action of monitoring and depends on the relevant communication rate, an impact from both the link of the suspicious transmitter to receiver and the link of the suspicious transmitter to the monitor.

Motivated by the above observations, intensive research efforts have been dedicated to securing the ISAC against target eavesdropping [17–21]. In [17] and [18], artificial noise was utilized for securing radar-communication systems with malicious targets. In [19], the sensing functionality of ISAC was capitalized on to estimate the directions of potential eavesdroppers, and the benefits of this method were validated by a weighted optimization of estimation accuracy and security. As for the STAR-RIS-empowered ISAC, the authors of [20] proposed a bi-directional sensing STAR-RIS to address the energy/signal leakage issue, and then minimized the Cramer-Rao bound by alternately optimizing sensing waveform, transmit power, and reflection-transmission coefficients.

However, the aforementioned studies focus on diagonal RISs in which each RIS element is connected to a single load disconnected from the others [22,23]. To mitigate this limitation, beyond diagonal (BD)-RIS has been proposed recently as a generalized RIS architecture, allowing for inter-element connections, among which the fully-connected (FC) RIS is a special case that offers the utmost beamforming gain with all elements of the RIS as the connected group [22]. Compared with the conventional single-connected RISs, the BD-RIS has greater structural flexibility since RIS elements can connected in various ways [23]. As its name suggests, the phase shift matrix in BD-RIS is no longer diagonal, offering new space for performance enhancements. Also, to achieve full-space wireless coverage and ubiquitous connectivity, the technology of simultaneous transmitting and reflecting RIS (STAR-RIS) was introduced [24]. Three protocols of STAR-RIS, namely energy-splitting (ES), mode-switching (MS), and time-switching (TS) were proposed, enabling STAR-RIS to transmit, reflect, or both simultaneously. Specifically, in the ES and MS protocols, the incident signal is split into two portions by the STAR-RIS. By contrast, a TS-based STAR-RIS exploits a switch to allocate separate time periods for its transmissions and reflections. Moreover, it was suggested that the BD-RISs could be well adapted to the hybrid mode of STAR-RIS [25], promising extended signal coverage and enhanced connectivity with more degrees of freedom. Despite the various research attempts that have been made on STAR-RIS or BD-RIS aided ISAC systems, the performance analysis is still in its infancy.

Moreover, none of the above works have integrated the BD-RIS with the TS-based STAR-RIS or proposed multiuser scheduling schemes in integrated sensing and multiuser communications (ISAMC) systems. Therefore, in this paper, we examine a STAR-FC-RIS-aided ISAMC system in the presence of target eavesdropping. The main contributions of this paper are summarized as follows. First of

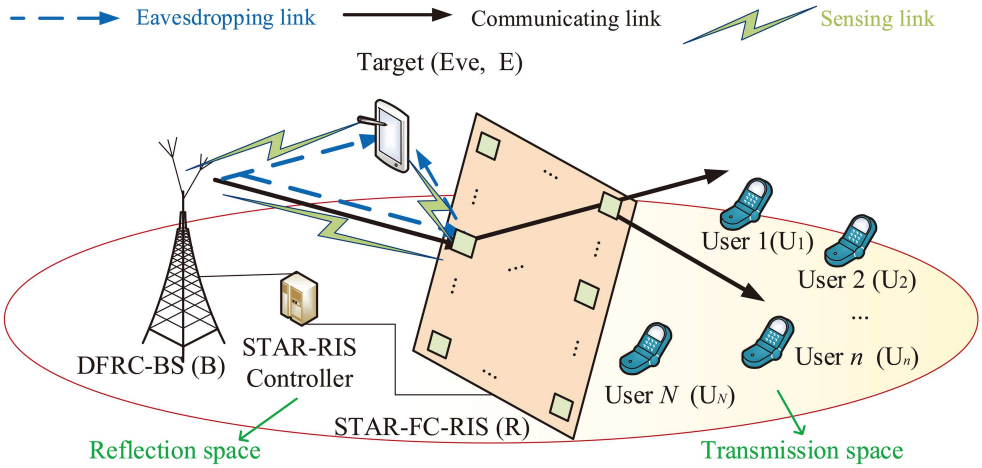

Figure 1 (Color online) The considered STAR-FC-RIS empowered ISAMC network in the presence of target eavesdropping.

all, we propose the simultaneous-transmitting-and-reflecting fully-connected RIS round-robin scheduling (STAR-FCR-RS) scheme and the simultaneous-transmitting-and-reflecting fully-connected RIS multiuser scheduling (STAR-FCR-MS) scheme to improve the security of downlink communications and derive closed-form expressions of the sensing outage probability (SOP), communications outage probability (COP), and communications intercept probability (CIP). In addition, a time optimization between transmission and reflection of the STAR-RIS is conducted to further improve the overall performance of STAR-FC-RIS-empowered ISAMC systems.

The rest of the paper is organized as follows. Section 2 describes the system model. In Section 3, we propose multiuser scheduling schemes and present a closed-form analysis of the schemes. Next, in Section 4, numerical results are presented. Finally, Section 5 concludes the paper.

Notations. $|\cdot|$ is used for the absolute value of a complex variable, $\mathbf{a}^{\mathrm{T}}$ and $\mathbf{a}^{\mathrm{H}}$ mean the transpose and conjugate transpose of vectors, respectively. Also, $\mathrm{diag}(\cdot)$ denotes a diagonal matrix, $\mathrm{E}(\cdot)$ represents statistical expectation operator, and $\arg(\cdot)$ represents the phase of a complex number, i.e., $a = |a|\arg(a)$. Besides, $n!$ represents factorial of a non-negative number n, and $\Gamma(\cdot,\cdot)$ represents the upper incomplete gamma function, where $\Gamma(\cdot) = \Gamma(\cdot, 0)$ is the gamma function, and $\Gamma(n+1) = n!$.

2 System model

In this section, we describe the adopted network model and the corresponding signal model of a STAR-FC-RIS aided ISAMC system, and present the considered performance metrics for sensing reliability, communications reliability, and communications security.

2.1 Network deployment

As illustrated in Figure 1, we consider a STAR-FC-RIS empowered ISAMC network consisting of a DFRC base station (BS), N users whose set is denoted by $\mathcal{U} \triangleq \{\mathrm{U}_1, \mathrm{U}_2, \cdots, \mathrm{U}_n, \cdots, \mathrm{U}_N\}$, an untrusted target, and a STAR-FC-RIS with L co-located elements, whose set is denoted by $\mathcal{R} \triangleq \{\mathrm{R}_1, \mathrm{R}_2, \cdots, \mathrm{R}_l, \cdots, \mathrm{R}_L\}$[1)]. In particular, the FC-RIS is a typical kind of BD-RIS architecture where all RIS elements are connected with tunable impedance components. Besides, all users are located at the other side of the STAR-RIS, and their downlink service is established by adopting time division multiple access (TDMA)-based opportunistic scheduling with channel pre-knowledge[2)]. This setup indicates that the users are in the vicinity of one another within a cluster but relatively space apart from the BS, which is different from most of the existing works focusing on the non-orthogonal multiple access (NOMA) systems. Since the users and BS are assumed to be at different sides of the STAR-FC-RIS, i.e., reflection space and transmission space, the degraded direct B-U_n links are ignored due to severe shadowing from a distance. Since the

1) We consider that each node is equipped with a single antenna, while our result can be extended to multi-antenna cases with a slight modification, which is left for future work.

2) To explore an upper bound of the sensing and communication security performance, we consider perfect CSI in this system model.

location of the sensing target is unknown, then a full-space connection with the BS can be boosted by a STAR-RIS. However, it acts as a potential eavesdropper and can adjust its location to wiretap more confidential information intended to secure users [15,16][3)]. Notably, the STAR-FC-RIS adopts the TS protocol, where we focus on the transmission and reflection of the STAR-FC-RIS in separate phases, while the MS protocol is also introduced in the sequel as numerical examples for comparison purposes. We assume sensing reliability and communications signals are designed to transmit in different phases, and $\tau_{\mathrm{T}} + \tau_{\mathrm{R}} = 1$ is satisfied for the TS protocol [26], where τ_{T} and τ_{R} denote the duty cycle taken up by the transmission and reflection, respectively.

2.2 Channel model

We assume Rayleigh fading channels between any two nodes (i.e., R, E, B, U_n), given by $\mathbf{h}_{\mathrm{RU}_n} \sim \mathcal{CN}\left(\mathbf{0}, \boldsymbol{\sigma}^2_{\mathrm{RU}_n}\right)$ and $\mathbf{h}_{\mathrm{RE}} \sim \mathcal{CN}\left(\mathbf{0}, \boldsymbol{\sigma}^2_{\mathrm{RE}}\right)$, where $\boldsymbol{\sigma}^2_{\mathrm{RU}_n} \in \mathbb{C}^L$ or $\boldsymbol{\sigma}^2_{\mathrm{BE}} \in \mathbb{C}^L$ represents a respective variance. We assume $\mathbf{h}_{\mathrm{RU}_n}$ and $\mathbf{h}_{\mathrm{RE}}$ are time-varying regarding the randomness of wireless channels. By contrast, $\mathbf{h}_{\mathrm{BR}}$ is regarded to be deterministic owing to its LoS without any blockage, i.e., $\mathbf{h}_{\mathrm{BR}} = \boldsymbol{\sigma}^2_{\mathrm{BR}}$, since the RIS is usually deployed near the BS with better channel condition of the BR link. The novelty of our system model lies in an integration of BD-RISs and STAR-RISs[4)]. We consider a novel BD-RIS architecture, where every port of the reconfigurable impedance network is fully connected to all other ports [27]. The fully-connected architecture offers the highest level of flexibility and optimization potential but comes with challenges in the tradeoff between beamforming capability and increased control complexity. Specifically, the transmission/reflection scattering coefficient matrices of the STAR-FC-RIS are not limited to be diagonal and are expressed as the following complex symmetric unitary matrix[5)]

$$\boldsymbol{\Theta}^{\mathrm{H}}_{\mathrm{T},\,n}\boldsymbol{\Theta}_{\mathrm{T},\,n} = \mathbf{I}_L,\ \boldsymbol{\Theta}_{\mathrm{T},\,n} = \boldsymbol{\Theta}^{\mathrm{T}}_{\mathrm{T},\,n}, \quad \forall n, \tag{1}$$

and

$$\boldsymbol{\Theta}^{\mathrm{H}}_{\mathrm{R}}\boldsymbol{\Theta}_{\mathrm{R}} = \mathbf{I}_L,\ \boldsymbol{\Theta}_{\mathrm{R}} = \boldsymbol{\Theta}^{\mathrm{T}}_{\mathrm{R}}, \tag{2}$$

where the "R" refers to the transmission and reflection modes, respectively. With the consideration of co-located elements of the STAR-FC-RIS, we consider the channels as independently and identically distributed (i.i.d.) from different reflecting elements of the STAR-FC-RIS, expressed as $\sigma^2_{\mathrm{BR}_l} \in \boldsymbol{\sigma}^2_{\mathrm{BR}} = \sigma^2_{\mathrm{BR}}, \mathrm{R}_l \in \mathcal{R}$.

2.3 Radar received signal

The target echo signal can be doubly enhanced by being reflected twice. Hence, although the propagation loss is doubled, the echo signal is strong enough to be collected at the BS. Then, a joint notation with dedicated radar-communication signals transmitted by the DFRC-BS is expressed as[6)]

$$x = \sqrt{P_{\mathrm{s}}}x_{\mathrm{s}} + \sqrt{P_{\mathrm{c}}}x_{\mathrm{c}}, \tag{3}$$

where x_{s} is the normalized sensing signal and x_{c} is the normalized communications signal. Also, P_{s} and P_{c} are the power allocated for sensing and communications, respectively. In this paper, we consider the equal power allocation, i.e., $P_{\mathrm{s}} = P_{\mathrm{c}}$, and an optimal power allocation can be left for future work. When the STAR-FC-RIS works in the reflection mode, the received radar signal at the BS can be expressed as

$$y^{\mathrm{R}}_{\mathrm{B}} = (h_{\mathrm{EB}} + \mathbf{h}^{\mathrm{H}}_{\mathrm{RB}}\boldsymbol{\Theta}_{\mathrm{R}}\mathbf{h}_{\mathrm{ER}})(h_{\mathrm{BE}} + \mathbf{h}^{\mathrm{H}}_{\mathrm{RE}}\boldsymbol{\Theta}_{\mathrm{R}}\mathbf{h}_{\mathrm{BR}})x + n_{\mathrm{B}}, \tag{4}$$

3) Without loss of generality, we regard the malicious target locates on the same side as the STAR-FC-RIS. By tracking the movement of the target, its location can be predicted based on previous estimates, and this knowledge can be utilized in STAR-FC-RIS deployment. If multiple legitimate users are in the reflection space of the STAR-RIS while a malicious radar target is in the transmission space, similar performance analysis as this model can be presented. Moreover, although we consider a single target in this paper, the results of the considered system model can be readily extended to multiple-target cases, where multiple targets can either work independently or collaboratively.

4) The BD-RIS extends the conventional RIS architecture by connecting different RIS elements with tunable impedance components and elevates the configuration flexibility.

5) Each element $l \in \mathcal{L}$ of the STAR-RIS is assumed to be independent. Although the phase-shift correlation of transmission and reflection are considered in some works, it is beyond the scope of this work, i.e., we adopt the independent phase-shift model without loss of generality.

6) Although separate transmissions lead to higher hardware cost, that also observes performance gain from power allocation.

from which the signal-to-interference-plus-noise ratio (SINR) is given by

$$\Lambda^{\mathrm{R}} = \frac{\gamma_{\mathrm{s}} \left| h_{\mathrm{EB}} + \mathbf{h}_{\mathrm{RB}}^{\mathrm{H}} \boldsymbol{\Theta}_{\mathrm{R}} \mathbf{h}_{\mathrm{ER}} \right|^2 \left| h_{\mathrm{BE}} + \mathbf{h}_{\mathrm{RE}}^{\mathrm{H}} \boldsymbol{\Theta}_{\mathrm{R}} \mathbf{h}_{\mathrm{BR}} \right|^2}{\eta \gamma_{\mathrm{c}} + 1} \overset{(a)}{=} \frac{\gamma_{\mathrm{s}} \left| h_{\mathrm{EB}} + \sqrt{\beta_{\mathrm{R}}} \mathbf{h}_{\mathrm{RB}}^{\mathrm{H}} \boldsymbol{\Theta}_{\mathrm{R}} \mathbf{h}_{\mathrm{ER}} \right|^4}{\eta \gamma_{\mathrm{c}} + 1}, \tag{5}$$

where $h_{\mathrm{EB}} \in \mathbb{C}$, $h_{\mathrm{BE}} \in \mathbb{C}$, $\mathbf{h}_{\mathrm{RB}} \in \mathbb{C}^{L \times 1}$, $\mathbf{h}_{\mathrm{BR}} \in \mathbb{C}^{L \times 1}$, $\mathbf{h}_{\mathrm{ER}} \in \mathbb{C}^{L \times 1}$, and $\mathbf{h}_{\mathrm{RE}} \in \mathbb{C}^{L \times 1}$ represent the channel fading coefficients of the E-BS, BS-E direct links and R-BS, BS-R, E-R, R-E reflecting links, respectively, $\gamma_{\mathrm{s}} = P_{\mathrm{s}}/N_0$ and $\gamma_{\mathrm{c}} = P_{\mathrm{c}}/N_0$. The equality of (a) in (5) holds upon the assumption of quasi-static block-fading channels with a slowly moving target. Thus, the wireless environments experienced by the signals of (E-BS, BS-E), (R-BS, BS-R), (E-R, R-E) are respectively formulated as reciprocal, with $\mathbf{h}_{\mathrm{RB}} = \mathbf{h}_{\mathrm{BR}}$ and $\mathbf{h}_{\mathrm{ER}} = \mathbf{h}_{\mathrm{RE}}$ [28, 29]. Both the forward and reverse sensing links share the same phase shift design of the two-way RIS. Besides, all receiving signals are equally deteriorated by an additive white Gaussian noise (AWGN) with a zero mean and N_0 variance, among which the AWGN at the BS is denoted as n_{B}. It is worth mentioning that the received information signal at the BS is equivalently regarded as self-interference (SI) and loop-interference (LI) from simultaneous transmitted and received signals in the same frequency caused by reflections of RIS. Since the communications signal is already known by the BS, typical estimations for channel gain of the reflecting links and reflection loss at the RIS can help to suppress the SI and LI, and is introduced as a random variable whose power is constant and proportional to the transmit power, i.e., $\eta \gamma_{\mathrm{c}} N_0$, where $\eta \in [0, 1]$ denotes the SI and LI cancellation level.

2.4 Communications received signal

The users take advantage of the transmission mode of the STAR-RIS to communicate. It is worth mentioning that the device-based ISAC considered in this paper leads to a shared hardware platform with a DFRC waveform and a joint transmit power. When x is transmitted by the DFRC-BS, at the n-th user denoted by U_n the received signal is given by

$$y_{\mathrm{U}_n} = (\mathbf{h}_{\mathrm{RU}_n}^{\mathrm{H}} \boldsymbol{\Theta}_{\mathrm{T},\, n} \mathbf{h}_{\mathrm{BR}}) x + n_{\mathrm{U}_n}, \tag{6}$$

where $\mathbf{h}_{\mathrm{BR}} \in \mathbb{C}^{L \times 1}$ and $\mathbf{h}_{\mathrm{RU}_n} \in \mathbb{C}^{L \times 1}$ represent downlink channel fading coefficients of the BS-R and R-U_n transmissions, respectively, and n_{U_n} is the AWGN at the n-th user. Due to the reuse of waveform, the mutual interference between the two functionalities is difficult to avoid. Combining (3) and (6), we obtain the data rate of the BS-U_n link as

$$R_{\mathrm{BU}_n} = \log_2 \left(1 + \frac{\gamma_{\mathrm{c}} |\mathbf{h}_{\mathrm{RU}_n}^{\mathrm{H}} \boldsymbol{\Theta}_{\mathrm{T},\, n} \mathbf{h}_{\mathrm{BR}}|^2}{\gamma_{\mathrm{s}} |\mathbf{h}_{\mathrm{RU}_n}^{\mathrm{H}} \boldsymbol{\Theta}_{\mathrm{T},\, n} \mathbf{h}_{\mathrm{BR}}|^2 + 1} \right). \tag{7}$$

By observing the broadcast nature of wireless propagation, the signals for the users can also be overheard by the malicious target, denoted by E, since the wiretap takes place through the sensing channel with the superposition of confidential information and detection signal. Analogous to (6), the received signal in the reflecting phase at the target is written as

$$y_{\mathrm{E}} = h_{\mathrm{BE}} x + n_{\mathrm{E}}, \tag{8}$$

from which the eavesdropping rate is given by

$$R_{\mathrm{BE}} = \log_2 \left(1 + \frac{\gamma_{\mathrm{c}} |h_{\mathrm{BE}}|^2}{\gamma_{\mathrm{s}} |h_{\mathrm{BE}}|^2 + 1} \right), \tag{9}$$

and n_{E} in (8) is the AWGN at the malicious target.

2.5 System performance indicators

Following the definition of performance indicators in the literatures [30–32], we observe a sensing outage event when the sensing SINR falls below a particular threshold λ_{th}, mathematically described as

$$P_{\mathrm{Sout}} = \tau_{\mathrm{R}} \Pr(\Lambda^{\mathrm{R}} < \lambda_{\mathrm{th}}), \tag{10}$$

namely sensing outage probability (SOP), where Λ^{R} is expressed as (5). By following the literature on performance analysis, the communications outage probability (COP) of the n-th user is expressed as

$$P_{\mathrm{Cout},\,n} = \tau_{\mathrm{T}} \Pr(R_{\mathrm{BU}_n} < R_0). \tag{11}$$

By following [33], an intercept event happens when the eavesdropping rate gets too high. Accordingly, we present the definition of the communications intercept probability (CIP) as

$$P_{\mathrm{Cint}} = \tau_{\mathrm{T}} \Pr(R_{\mathrm{BE}} > R_0 - R_{\mathrm{s}}), \tag{12}$$

where R_{s} is a secrecy threshold. All probabilities facilitate a unified metric for ISAC, namely sensing-communication probability (SCP) [34–36], defined by the mean of SOP, COP, and CIP as

$$P_{\mathrm{SC},\,n} = (P_{\mathrm{Sout}} + P_{\mathrm{Cout},\,n} + P_{\mathrm{Cint}})/3, \tag{13}$$

which reveals the sensing/communications tradeoff, since the three probabilities of sensing outage probability, communications outage probability, and communications intercept probability inside the SCP definition must be balanced. Otherwise, the SCP increases because of sensing outage events or communications outage/intercept ones.

3 Proposed multiuser scheduling schemes and performance analysis

In this section, we propose the energy-splitting (STAR-FCR) schemes with round-robin scheduling and multiuser scheduling, and then carry out the SOP, CIP, and COP analysis in closed forms.

3.1 Equivalent channels of FC-RIS-aided communications

We denote the average gain of the cascaded channels of the STAR-FC-RIS aided B-U$_n$ links as $W_n = ||\mathbf{h}_{\mathrm{BR}}||^2||\mathbf{h}_{\mathrm{RU}_n}||^2 \overset{(b)}{=} L\sigma_{\mathrm{BR}}^2 \sum_{l=1}^{L} |h_{\mathrm{R}_l\mathrm{U}_n}|^2$, where the equality (b) holds with the optimal phase shifts, presented in the sequel. Then, we obtain the cumulative density function (CDF) of W_n as

$$\Pr(W_n \leqslant w) = 1 - \frac{\Gamma(L, \frac{w}{L\sigma_{\mathrm{BR}}^2\sigma_{\mathrm{RU}_n}^2})}{\Gamma(L)}, \quad \forall \mathrm{U}_n \in \mathcal{U}. \tag{14}$$

By denoting $S \overset{(c)}{=} L\sigma_{\mathrm{BR}}^2 \sum_{l=1}^{L} |h_{\mathrm{R}_l\mathrm{E}}|^2$ where the equality (c) holds relying on co-phase alignments of the FC-RIS both in the transmission phase and reflection phase [25].

Taking the transmitting phase with no direct downlinks for instance, by utilizing the eigenvalues decomposition, $\mathbf{\Theta}_{\mathrm{T},\,n}$ in (1) can be equivalently written as

$$\mathbf{\Theta}_{\mathrm{T},\,n} = \mathbf{V}\mathbf{D}_{\mathrm{T},\,n}\mathbf{V}^{\mathrm{T}}, \quad \forall n, \tag{15}$$

where $\mathbf{D}_{\mathrm{T},\,n}$ is a diagonal matrix given by $\mathbf{D}_{\mathrm{T},\,n} = \mathrm{diag}([\mathrm{e}^{-j\phi_{n,1}^{\mathrm{T}}}, \cdots, \mathrm{e}^{-j\phi_{n,l}^{\mathrm{T}}}, \cdots, \mathrm{e}^{-j\phi_{n,L}^{\mathrm{T}}}])$, wherein $\phi_{n,l}^{\mathrm{T}} \in [0, 2\pi)$ denotes the phase shift induced by the l-th FC-RIS element. Note that the channel gain given in (7) can be expanded using the Cauchy-Schwarz inequality as

$$|\hat{\mathbf{h}}_{\mathrm{R}n}^{\mathrm{H}}\mathbf{D}_{\mathrm{T},\,n}\hat{\mathbf{h}}_{\mathrm{BR}}|^2 \leqslant \|\hat{\mathbf{h}}_{\mathrm{BR}}^{\mathrm{H}}\|^2\|\mathbf{D}_{\mathrm{T},\,n}\hat{\mathbf{h}}_{\mathrm{R}n}\|^2, \quad \forall n, \tag{16}$$

where $\hat{\mathbf{h}}_{\mathrm{BR}}^{\mathrm{H}} = \mathbf{h}_{\mathrm{BR}}^{\mathrm{H}}\mathbf{V}$, $\hat{\mathbf{h}}_{\mathrm{R}n} = \mathbf{V}^{\mathrm{T}}\mathbf{h}_{\mathrm{R}n}$ and the equality is achieved when the desired phase shifts introduced by the STAR-FC-RIS should align with the cascaded channel coefficients as to maximize the average gain given by

$$\phi_{n,l} = -\arg([\mathbf{h}_{\mathrm{BR}}\mathbf{V}]_l) - \arg([\mathbf{V}^{\mathrm{T}}\mathbf{h}_{\mathrm{R}n}]_l), \quad \forall l, \tag{17}$$

where by following Algorithm 1 [27], $\mathbf{V}$ can be obtained for fully-connected RIS in single-user SISO systems, provided in Algorithm 1. As for the reflecting phase with a direct link, the optimal phase shift can be likewise designed as

$$\phi_{n,l}^{\mathrm{R}} = \arg(h_{\mathrm{BE}}) - \arg([\mathbf{h}_{\mathrm{BR}}\mathbf{V}]_l) - \arg([\mathbf{V}^{\mathrm{T}}\mathbf{h}_{\mathrm{R}n}]_l), \quad \forall l. \tag{18}$$

Algorithm 1 Obtaining $\mathbf{V}$ for the optimal phase shift design of FC-RIS-aided SISO systems

Input: $\mathbf{h}_{\mathrm{RU}_n} \in \mathbb{C}^{L\times 1}, \mathbf{h}_{\mathrm{BR}} \in \mathbb{C}^{L\times 1}$;

Output: $\mathbf{h}_{\mathrm{RU}_n} \in \mathbb{C}^{L\times 1}, \mathbf{h}_{\mathrm{BR}} \in \mathbb{C}^{L\times 1}$; Set $\mathbf{R}_{\mathrm{RU}_n} = \mathbf{h}_{\mathrm{RU}_n}^{\mathrm{H}}\mathbf{h}_{\mathrm{RU}_n}, \mathbf{R}_{\mathrm{BR}} = \mathbf{h}_{\mathrm{BR}}\mathbf{h}_{\mathrm{BR}}^{\mathrm{H}}$; $\mathbf{A}_{\mathrm{RU}_n} = \frac{\mathbf{R}_{\mathrm{RU}_n}+\mathbf{R}_{\mathrm{RU}_n}^{\mathrm{T}}}{2}, \mathbf{A}_{\mathrm{BR}} = \frac{\mathbf{R}_{\mathrm{BR}}+\mathbf{R}_{\mathrm{BR}}^{\mathrm{T}}}{2}$; $\mathbf{A} \triangleq \mathbf{U}\mathbf{D}\mathbf{U}^{\mathrm{T}} = \mathbf{A}_{\mathrm{RU}_n} - \mathbf{A}_{\mathrm{BR}}$; $\delta = \mathrm{diag}(\mathbf{D}) \triangleq [\delta_1, \ldots, \delta_L]^{\mathrm{T}}$;

If $L == 2$ then $\mathbf{T} = \begin{bmatrix} \sqrt{\frac{1}{2}} & \sqrt{\frac{1}{2}} \\ \sqrt{\frac{1}{2}} & -\sqrt{\frac{1}{2}} \end{bmatrix}$;

Else if $L == 3$ then $\mathbf{T} = \begin{bmatrix} \sqrt{\frac{-\delta_3}{\delta_1-\delta_3}} & \sqrt{\frac{\delta_1}{2(\delta_1-\delta_3)}} & -\sqrt{\frac{\delta_1}{2(\delta_1-\delta_3)}} \\ 0 & \sqrt{\frac{1}{2}} & \sqrt{\frac{1}{2}} \\ \sqrt{\frac{\delta_1}{\delta_1-\delta_3}} & -\sqrt{\frac{-\delta_3}{2(\delta_1-\delta_3)}} & \sqrt{\frac{-\delta_3}{2(\delta_1-\delta_3)}} \end{bmatrix}$;

Else $\mathbf{t}_1 = \left[\sqrt{\frac{-\delta_{L-1}}{\delta_1-\delta_{L-1}}}, 0, \ldots, \sqrt{\frac{\delta_1}{\delta_1-\delta_{L-1}}}, 0\right]^{\mathrm{T}}$; $\mathrm{t}_2 = \left[0, \sqrt{\frac{-\delta_L}{\delta_2-\delta_L}}, \ldots, 0, \sqrt{\frac{\delta_2}{\delta_2-\delta_L}}\right]^{\mathrm{T}}$; $\mathrm{t}_3 = \frac{1}{\sqrt{2}}\left[[\mathrm{t}_1]_{L-1}, [\mathrm{t}_2]_L, \ldots, -[\mathrm{t}_1]_1, -[\mathrm{t}_2]_2\right]^{\mathrm{T}}$; $\mathrm{t}_4 = \frac{1}{\sqrt{2}}\left[[\mathrm{t}_1]_{L-1}, -[\mathrm{t}_2]_L, \ldots, -[\mathrm{t}_1]_1, [\mathrm{t}_2]_2\right]^{\mathrm{T}}$; $\mathbf{T} = [\mathbf{t}_1, \mathbf{t}_2, \mathbf{t}_3, \mathbf{t}_4, \mathbf{e}_3, \ldots, \mathbf{e}_{N-2}]$;

Return The optimal solution $\mathbf{V} = \mathbf{U}\mathbf{T}$.

With the optimal phase shifts and letting $U = \left|\sqrt{S} + |h_{\mathrm{EB}}|\right|^2$, we obtain the CDF of U as

$$F_U(u) = \int_0^{\sqrt{u}} (1 - \mathrm{e}^{-\frac{(\sqrt{u}-s)^2}{\sigma_{\mathrm{BE}}^2}}) \mathrm{e}^{-\frac{s^2}{L\sigma_{\mathrm{BR}}^2\sigma_{\mathrm{RE}}^2}} \frac{s^{2L-1}}{L!\sigma_{\mathrm{BR}}^{2L}\sigma_{\mathrm{RE}}^{2L}} \mathrm{d}s. \tag{19}$$

which can be derived using the Taylor extension as

$$F_U(u) = 1 - \sum_{m=0}^{L-1} \frac{u^m}{m!L^m\sigma_{\mathrm{BR}}^{2m}\sigma_{\mathrm{RE}}^{2m}} \mathrm{e}^{-\frac{u}{L\sigma_{\mathrm{BR}}^2\sigma_{\mathrm{RE}}^2}} + \sum_{n=0}^{\infty} \int_0^{\sqrt{u}} \frac{(-1)^{n+1}(\sqrt{u}-s)^{2n}s^{2L-1}}{L!n!\sigma_{\mathrm{RE}}^{2L}\sigma_{\mathrm{BR}}^{2L}\sigma_{\mathrm{BE}}^{2n}} \mathrm{e}^{-\frac{s^2}{L\sigma_{\mathrm{BR}}^2\sigma_{\mathrm{RE}}^2}} \mathrm{d}s, \tag{20}$$

which can be then calculated with the help of [37, Eq. (3.478.3)].

3.2 SOP/CIP analysis of the STAR-FC-RIS-aided schemes

Since the sensing process involves an untrusted target instead of all users, the SOP derived in this subsection can be applicable for both the STAR-FCR-RS and STAR-FCR-MS schemes. Letting $Q = \lambda_{\mathrm{th}} - |h_{\mathrm{EB}}|$, we obtain the closed-form SOP of the STAR-FC-RIS aided ISAC system as

$$P_{\mathrm{Sout}} = F_U(\lambda_{\mathrm{th}}) = \Pr(\sqrt{S} < Q). \tag{21}$$

By capitalizing on (20), we obtain

$$\begin{aligned} P_{\mathrm{Sout}} = \tau_{\mathrm{R}}\Bigg(1 - \sum_{m=0}^{L-1} \frac{\lambda_{\mathrm{th}}^m}{m!L^m\sigma_{\mathrm{RE}}^{2m}\sigma_{\mathrm{BR}}^{2m}} \mathrm{e}^{-\frac{\lambda_{\mathrm{th}}}{L\sigma_{\mathrm{BR}}^2\sigma_{\mathrm{RE}}^2}} + \sum_{n=0}^{\infty} \frac{(-1)^{n+1}}{\sigma_{\mathrm{BE}}^{2n}} \mathcal{B}(2n-2L+1, 2L-1) \\ \times \lambda_{\mathrm{th}}^{n-\frac{1}{2}} {}_2F_2\left(\tfrac{2L-1}{2}, L; n, n+\tfrac{1}{2}; -\tfrac{\lambda_{\mathrm{th}}}{L\sigma_{\mathrm{BR}}^2\sigma_{\mathrm{RE}}^2}\right)\Bigg), \end{aligned} \tag{22}$$

where $\mathcal{B}(\cdot,\cdot)$ is the beta function defined as [37, Eq. (8.382)], ${}_pF_q(\cdot)$ represents the generalized hypergeometric function [37, Eq.(9.210.1)] with "p" and "q" denoting the orders, respectively. Likewise, the closed-form CIP of the STAR-FC-RIS-aided ISAC system can be given by

$$\begin{aligned} P_{\mathrm{Cint}} =& \tau_{\mathrm{T}}\Bigg[\sum_{n=0}^{\infty} \frac{(-1)^{n+1}}{\sigma_{\mathrm{BE}}^{2n}} \mathcal{B}(2n-2L+1, 2L-1) \left[\frac{2^{R_0-R_{\mathrm{s}}}-1}{\gamma_{\mathrm{c}} - (2^{R_0-R_{\mathrm{s}}}-1)\gamma_{\mathrm{s}}}\right]^{n-\frac{1}{2}} \\ & {}_2F_2\left(\frac{2L-1}{2}, L; n, n+\frac{1}{2}; -\frac{2^{R_0-R_{\mathrm{s}}}-1}{[\gamma_{\mathrm{c}} - (2^{R_0-R_{\mathrm{s}}}-1)\gamma_{\mathrm{s}}]L\sigma_{\mathrm{BR}}^2\sigma_{\mathrm{RE}}^2}\right) \\ & + 1 - \sum_{m=0}^{L-1} \frac{(2^{R_0-R_{\mathrm{s}}}-1)^m}{[\gamma_{\mathrm{c}} - (2^{R_0-R_{\mathrm{s}}}-1)\gamma_{\mathrm{s}}]^m m!L^m\sigma_{\mathrm{BR}}^{2m}\sigma_{\mathrm{RE}}^{2m}} \mathrm{e}^{-\frac{2^{R_0-R_{\mathrm{s}}}-1}{[\gamma_{\mathrm{c}} - (2^{R_0-R_{\mathrm{s}}}-1)\gamma_{\mathrm{s}}]L\sigma_{\mathrm{BR}}^2\sigma_{\mathrm{RE}}^2}}\Bigg]. \end{aligned} \tag{23}$$

3.3 COP of the STAR-FCR-RS scheme

In this section, we present the STAR-FCR-RS scheme as a baseline, where the users are allowed to orderly access the downlink channels slot-by-slot. In the STAR-FCR-RS scheme, the overall COP of the multiuser system can be written as

$$P_{\text{Cout, STAR-FCR-RS}} = \frac{1}{N}\sum_{n=1}^{N} P_{\text{Cout, }n}, \tag{24}$$

where $P_{\text{Cout},n}$ is expressed as (11). Then, the closed-form COP of the STAR-FCR-RS scheme can be obtained as

$$P_{\text{Cout, STAR-FCR-RS}} = \tau_{\text{T}}\left(1 - \frac{1}{N}\sum_{n=1}^{N}\frac{\Gamma\left(L, \frac{2^{R_0}-1}{[\gamma_{\text{c}}-(2^{R_0}-1)\gamma_{\text{s}}]L\sigma^2_{\text{BR}}\sigma^2_{\text{RU}_n}}\right)}{\Gamma(L)}\right). \tag{25}$$

3.4 COP of the STAR-FCR-MS scheme

In this section, we propose the STAR-FCR-MS scheme, where opportunistic scheduling is performed according to the channel pre-knowledge of downlink transmission to improve the secrecy rate. Specifically, in each time slot, the user with the highest main channel gain is chosen by following the criterion as

$$o = \arg\max_{\text{U}_n\in\mathcal{U}}\{W_n\}, \tag{26}$$

where the CSI of downlink channels can be more available than the eavesdropping channels. With the STAR-FCR-MS scheme adopted, the closed-form expression of the overall COP of the multiuser system can be written as

$$P_{\text{Cout, STAR-FCR-MS}} = \tau_{\text{T}}\text{F}_{W_o}(w_1) = \tau_{\text{T}}\prod_{\text{U}_n\in\mathcal{U}}\text{F}_{W_n}(w_1), \tag{27}$$

where $w_1 = \frac{2^{R_0}-1}{[\gamma_{\text{c}}-(2^{R_0}-1)\gamma_{\text{s}}]L\sigma^2_{\text{BR}}\sigma^2_{\text{RU}_n}}$. Then, the CDF of W_o can be further derived by capitalizing on the generalized multinomial theorem as

$$\text{F}_{W_o}(w_1) = 1 + \sum_{\text{U}_n\in J_q,\, q=1}^{2^N-1}(-1)^{|J_q|}\text{e}^{-\frac{|J_q|}{L\sigma^2_{\text{BR}}\sigma^2_{\text{RU}_n}}}\sum_{\mathcal{S}}\frac{A_1}{(L\sigma^2_{\text{BR}}\sigma^2_{\text{RU}_n})^{B_1}}, \tag{28}$$

where J_q represents the q-th non-empty subcollection of the user set $\mathcal{U}$, $|J_q|$ denote the cardinality of the set J_q, the set $\mathcal{S} = \{(n_1, n_2, \ldots, n_{k_1})\,|\,\sum_{p=1}^{k_1} n_p = |J_q|\}$, $A_1 = \frac{\prod_{k=1}^{k_1}\frac{1}{((k-1)!)^{n_k}}}{\prod_{p=1}^{k_1} n_p!}$, $B_1 = \sum_{p=1}^{k_1} n_p(p-1)$. Substituting (28) into (27) yields the closed-form COP of the STAR-FCR-RS scheme.

4 Numerical results and discussions

In this section, we present simulation results to verify the closed-form analysis as well as to demonstrate the performance gains achieved by the proposed schemes. Also, to show the ISAC performance tradeoff from a change of relative channel quality, we define the ratio of average gains between the main channel and eavesdropping channel, referred to as the main-to-eavesdropping ratio (MER) and denoted as $\zeta_{\text{MER}} = \frac{\sigma^2_{\text{RU}_n}}{\sigma^2_{\text{RE}}}$, where the parameters specified numerically are listed in Table 1, unless otherwise stated.

Moreover, the proposed STAR-FCR-RS and STAR-FCR-MS schemes observe respective SINR degradations due to the mutual interference brought by the two functionalities. To this end, based on the closed-form analysis, we carry out optimization analysis of the STAR-FCR-RS and STAR-FCR-MS schemes by minimizing SCP, i.e., the mean of SOP, COP, and CIP, with an optimized time allocation (OTA) of the STAR-FC-RIS, namely the STAR-FCR-RS-OTA and STAR-FCR-MS-OTA schemes. To summarize, all benchmark schemes are listed as follows.

Table 1 Simulation parameters

Description	Symbols	Values
The variances of direct-link channel fading coefficients	$\sigma^2_{\mathrm{BU}_n}$	1
The variances of reflective-link channel fading coefficients	$\sigma^2_{\mathrm{RU}_n}$	2
The transmit power at the DFRC BS for a separate signal	$\frac{P_{\mathrm{s}}}{N_0}, \frac{P_{\mathrm{c}}}{N_0}$	10 dB
MER	ζ_{MER}	10 dB, 0 dB
The number of STAR-RIS elements	L	16
The transmission/reflection coefficient of the STAR-FCR-based STAR-RIS	β_{T}, β_{R}	0.7, 0.3
The time allocation factor of the TS-based STAR-RIS	τ_{T}, τ_{R}	0.3, 0.7
Self interference and loop interference cancelation level	η	0.01

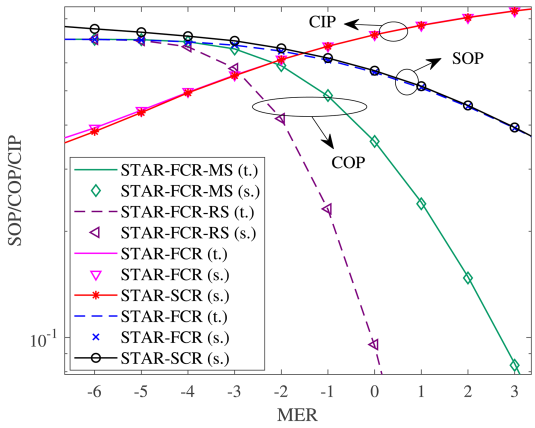

Figure 2 (Color online) The SOPs, CIPs, and COPs of the STAR-FCR-RS and STAR-FCR-MS schemes versus MER, where "t." and "s." stand for theoretical and simulation results, respectively.

(1) STAR-SCR: To highlight the performance superiority of the corresponding proposed STAR-FCR-RS and STAR-FCR-MS schemes, we replace the fully-connected BD-RIS with conventional single-connected one, with no connections between each element of RIS. Besides, the performance gaps between STAR-SCR-RS and STAR-SCR-MS schemes validate the secrecy benefits of multiuser scheduling.

(2) MSSTAR-FCR-MS: For comparison purposes, the MS protocol with simultaneous sensing and communications is also introduced to reveal the performance tradeoffs between sensing and communications. The FC-RIS can be considered to simultaneously transmit and reflect with TS or MS protocol[7)].

(3) D-FCR: In these double-RIS aided schemes, the full-space coverage facilitated by the STAR-RIS is achieved by employing a conventional pure-reflection FC-RIS and a pure-transmission FC-RIS. The two conventional RISs are deployed adjacent to each other at the same location as the STAR-RIS. For a fair comparison, each conventional reflecting/transmitting RIS is assumed to have $L/2$ elements, where L is assumed to be an even number.

(4) STAR-FCR-ETA: To highlight the performance superiority of the corresponding proposed STAR-FCR-RS-OTA and STAR-FCR-MS-OTA schemes, we also consider phases with equal time in the considered TS protocol. Since the user communications and target sensing are enhanced by the transmission and reflection of the STAR-FC-RIS, respectively, a time allocation between transmission and reflection modes strikes a tradeoff between sensing reliability, communications reliability, and communications security to improve the overall performance of the STAR-FC-RIS empowered ISAMC systems. In the two schemes above, the time is allocated with a fixed factor, 0.5, i.e., the system has equal time for transmission and reflection of the STAR-FC-RIS. As can be found, the further proposed STAR-FCR-RS-OTA and STAR-FCR-MS-OTA schemes are more adaptive with better performance, where an optimal transmission-coefficient is decided based on the statistical CSI.

Figure 2 plots the SOPs, CIPs, and COPs of the STAR-FCR-RS and STAR-FCR-MS schemes versus MER with solid lines (theoretical expressions) and discrete markers (Monte-Carlo simulations), whose well agreements verify our closed-form analysis. Also, corresponding performances of the STAR-SCR-RS and STAR-SCR-MS are shown for comparison purposes. The increasing MER means the stronger channel gains of the main channels compared with the eavesdropping channels. The crossings appear between the

7) In [25], the ES-based STAR-RIS was identified as a special variant of BD-RIS, namely the "cell-wise single-connected" model.

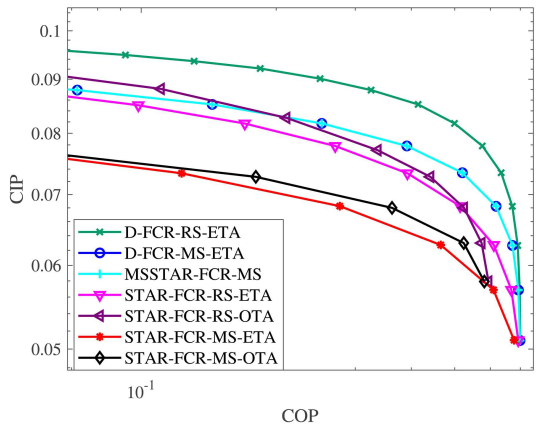

Figure 3 (Color online) The communication SRT performance of the STAR-FCR-RS-OTA and STAR-FCR-MS-OTA schemes and their benchmarks.

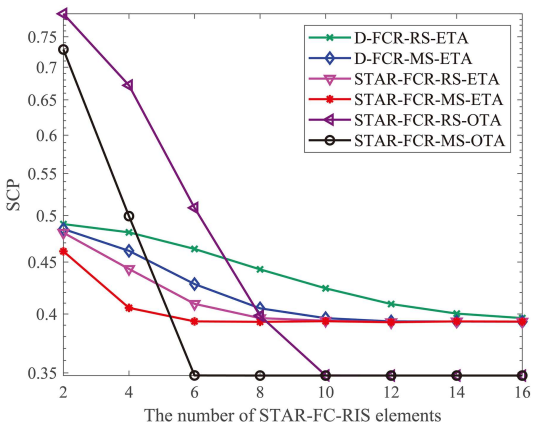

Figure 4 (Color online) The SCPs versus the number of STAR-FC-RIS elements.

SOPs or COPs and CIPs curves of respective schemes. This is because when the target eavesdropping is weakened in a wireless environment, the sensing is very likely to suffer a declined reliability due to the shared channels, so as the communications reliability. In a system where both reliability and security are of equal importance, the crossings represent the respective maximum acceptable error probabilities, underscoring a tradeoff between competing requirements. It can also be observed from Figure 2 that the implementation of an FC-RIS remarkably improves reliability while offering marginal security benefits, compared with a conventional SC-RIS. This motivates us to define SCP, a mean probability, to guarantee SOP/COP/CIP both low enough.

From Figure 3, we observe the CIP and COP performance tradeoff of the STAR-FCR-RS-OTA and STAR-FCR-MS-OTA schemes. The CIPs of all schemes fall as their COPs increase, and vice versa. This implies that the assistance of STAR-RIS improves the transmission of the users at the cost of degraded security, showing a tradeoff between communication security and reliability in each scheme. This is associated with the fact that an extended time duration for the transmission of STAR-RIS limits the time available for the reflecting mode to enhance sensing. To ensure the sensing reliability, strengthened power is required for the sensing, raising eavesdropping threats and leading to a worse secrecy performance. Along with the respective STAR-FCR-RS-ETA and STAR-FCR-MS-ETA schemes, the curves of STAR-FCR-RS-OTA and STAR-FCR-MS-OTA schemes are below that of other schemes, exhibiting better performance relying on their effective exploitation of CSI pre-knowledge, without considering the overhead to acquire CSI. Moreover, compared with the STAR-FCR-ETA schemes, the curves of STAR-FCR-OTA schemes decrease rapidly, only showing performance superiorities in the high MER region. The transmission or reflection mode of the STAR-BD-RIS depends on whether the user is at the transmission or reflection side, which requires high synchronization implementation complexity as the usual case in the TS protocol of STAR-RISs, but presents better performance than the MSSTAR-FCR-MS scheme. Since we optimize the power allocation or time allocation by exploiting statistical CSI, the double-RIS schemes perform the same as MSSTAR-aided schemes [38].

Figure 4 shows the SCPs versus the number of STAR-RIS elements. In the STAR-FCR-RS and STAR-FCR-MS schemes, we utilize the aforementioned tradeoff between communication security and sensing reliability and further carry out an iterative optimization analysis exploiting the optimal allocation factors of the STAR-RIS. With an increasing number of STAR-RIS elements, the mean of SOPs and OPs of all schemes decrease accordingly. It can be known from Figure 4 that, the more rapid decreases of the mean of SOPs and OPs indicate that an optimal allocation factor of the STAR-RIS helps the system make better use of the power resources, indicating the overall performance gain considering both sensing and communications. Indeed, from Figure 4, the outperformances of STAR-FCR-MS and TS-MS schemes validate the benefits of the MS compared with the conventional RS. Furthermore, the optimal time allocations have the proposed schemes converging to a lower floor in the sufficiently large number of RIS elements.

5 Conclusion

In this paper, we studied a STAR-FC-RIS aided ISAMC system in the presence of target eavesdropping, where a STAR-FC-RIS achieved enhancements of DFRC signals and target intercepting, highlighting the performance tradeoff between sensing/communication outage and communication security. We first presented closed-form analysis for the defined SCP of the STAR-FCR-RS scheme and the STAR-FCR-MS scheme, and then carried out optimization analyses of the time allocation for a TS-based STAR-FC-RIS exploiting statistical CSI, extensively improving the overall performance of STAR-FC-RIS-empowered ISAMC systems with effective utilization of the network energy resources.

Acknowledgements This work was supported in part by National Natural Science Foundation of China (Grant Nos. 62271268, 62071253, 62371252), National Science Fund for Distinguished Young Scholars of China (Grant No. 62125203), Jiangsu Provincial Key Research and Development Program (Grant No. BE2022800), Jiangsu Provincial 333 Talent Project, and the Open Research Fund of Key Laboratory of Broadband Wireless Communication and Sensor Network Technology (Nanjing University of Posts and Telecommunications) (Grant No. JZNY202303).

References

1 Cui Y, Liu F, Jing X, et al. Integrating sensing and communications for ubiquitous IoT: applications, trends, and challenges. IEEE Netw, 2021, 35: 158–167
2 Zhu G, Lyu Z, Jiao X, et al. Pushing AI to wireless network edge: an overview on integrated sensing, communication, and computation towards 6G. Sci China Inf Sci, 2023, 66: 130301
3 Liu Z P, Li X, Ji H, et al. Toward STAR-RIS-empowered integrated sensing and communications: joint active and passive beamforming design. IEEE Trans Veh Tech, 72: 15991–16005
4 Hua M, Wu Q, Chen W, et al. Secure intelligent reflecting surface-aided integrated sensing and communication. IEEE Trans Wireless Commun, 2024, 23: 575–591
5 Liu X, Huang T, Shlezinger N, et al. Joint transmit beamforming for multiuser mimo communications and mimo radar. IEEE Trans Signal Process, 2020, 68: 3929–3944
6 He Y, Cai Y, Mao H, et al. RIS-assisted communication radar coexistence: joint beamforming design and analysis. IEEE J Sel Areas Commun, 2022, 40: 2131–2145
7 Xu J, Yuen C, Huang C, et al. Reconfiguring wireless environments via intelligent surfaces for 6G: reflection, modulation, and security. Sci China Inf Sci, 2023, 66: 130304
8 Qian X, Hu X, Liu C, et al. Sensing-based beamforming design for joint performance enhancement of RIS-aided ISAC systems. IEEE Trans Commun, 2023, 71: 6529–6545
9 Meng K, Wu Q, Chen W, et al. Sensing-assisted communication in vehicular networks with intelligent surface. IEEE Trans Veh Technol, 2024, 73: 876–893
10 Wang C, Wang C C, Li Z, et al. STAR-RIS-enabled secure dual-functional radar-communications: joint waveform and reflective beamforming optimization. IEEE Trans Inform Forensic, 2023, 18: 4577–4592
11 Chu J, Lu Z, Liu R, et al. Joint beamforming and reflection design for secure RIS-ISAC systems. IEEE Trans Veh Technol, 2024, 73: 4471–4475
12 Zhang H, Zheng J. IRS-assisted secure radar communication systems with malicious target. IEEE Trans Veh Technol, 2024, 73: 591–604
13 Sun Y F, An K, Li C, et al. Joint transmissive and reflective RIS-aided secure MIMO systems design under spatially-correlated angular uncertainty and coupled PSEs. IEEE Trans Inf Forensic Secur, 18: 3606–3621
14 Hussain B, Du Q, Sun B, et al. Deep learning-based DDoS-attack detection for cyber-physical system over 5G network. IEEE Trans Ind Inf, 2021, 17: 860–870
15 Zou Y L, Zhu J, Li X L, Hanzo L. Relay selection for wireless communications against eavesdropping: a security-reliability trade-off perspective. IEEE Netw, 2016, 30: 74–79
16 Wang K, Lei H, Pan G, et al. Detection performance to spatially random UAV using the ground vehicle. IEEE Trans Veh Technol, 2020, 69: 16320–16324
17 Su N, Liu F, Masouros C. Secure radar-communication systems with malicious targets: integrating radar, communications and jamming functionalities. IEEE Trans Wireless Commun, 2021, 20: 83–95
18 Bazzi A, Chafii M. Secure full duplex integrated sensing and communications. IEEE Trans Inform Forensic, 2024, 19: 2082–2097
19 Su N, Liu F, Masouros C. Sensing-assisted eavesdropper estimation: an ISAC breakthrough in physical layer security. IEEE Trans Wireless Commun, 2024, 23: 3162–3174
20 Zhang Z, Liu Y, Wang Z, et al. STARS-ISAC: how many sensors do we need? IEEE Trans Wireless Commun, 2024, 23: 1085–1099
21 Su N, Liu F, Wei Z, et al. Secure dual-functional radar-communication transmission: exploiting interference for resilience against target eavesdropping. IEEE Trans Wireless Commun, 2022, 21: 7238–7252
22 Li H, Shen S, Clerckx B. A dynamic grouping strategy for beyond diagonal reconfigurable intelligent surfaces with hybrid transmitting and reflecting mode. IEEE Trans Veh Technol, 2023, 72: 16748–16753
23 Lin S Y, Zou Y L, Jiang Y H, et al. Securing FC-RIS and UAV empowered multiuser communications against aerial eavesdropping. 2024. arXiv:2408.14261
24 Liu Y W, Mu X D, Xu J Q, et al. STAR: Simultaneous transmission and reflection for 360 coverage by intelligent surfaces. IEEE Wireless Commun, 2021, 28: 102–109
25 Li H, Shen S, Clerckx B. Beyond diagonal reconfigurable intelligent surfaces: from transmitting and reflecting modes to single-, group-, and fully-connected architectures. IEEE Trans Wireless Commun, 2023, 22: 2311–2324
26 Xiao H, Hu X, Mu P, et al. Simultaneously transmitting and reflecting RIS (STAR-RIS) assisted multi-antenna covert communication: analysis and optimization. IEEE Trans Wireless Commun, 2024, 23: 6438–6452
27 Nerini M, Shen S P, Clerckx B. Closed-form global optimization of beyond diagonal reconfigurable intelligent surfaces. IEEE Trans. Wireless Commun, 2023, 2: 1037–1051

28 Liu R, Li M, Liu Y, Wu Q Q, et al. Joint transmit waveform and passive beamforming design for RIS-aided DFRC systems. IEEE J. Sel. Topics in Signal Processing, 2016, 5: 995–1010

29 Hua M, Wu Q Q, Chen W, et al. Secure intelligent reflecting surface-aided integrated sensing and communication. IEEE Trans. Wireless Commun, 2023, 1: 575–591

30 Salem A A, Ismail M H, Ibrahim A S. Active reconfigurable intelligent surface-assisted MISO integrated sensing and communication systems for secure operation. IEEE Trans Veh Technol, 2023, 72: 4919–4931

31 Lei H, Gao C, Ansari I S, et al. On physical layer security over SIMO generalized-K fading channels. IEEE Trans Veh Technol, 2016, 65: 7780–7785

32 Peng Z, Liu X, Liu X, et al. Performance analysis of active RIS-aided multi-pair full-duplex communications with spatial correlation and imperfect CSI. Sci China Inf Sci, 2023, 66: 192304

33 Feng Y H, Yan S H, Yang Z, et al. TAS-based incremental hybrid decode-amplify-forward relaying for physical layer security enhancement. IEEE Trans Commun, 2022, 21: 6861–6876

34 Lin S, Zou Y, Li B, et al. Security-reliability trade-off analysis of RIS-aided multiuser communications. IEEE Trans Veh Technol, 2023, 72: 6225–6237

35 Yan P, Ji X, Zou Y, et al. Physical-layer security for energy-harvesting multiuser systems under hardware impairments and channel estimation errors. IEEE Trans Green Commun Netw, 2024, 8: 656–671

36 Liu M, Yang M, Li H, et al. Performance analysis and power allocation for cooperative ISAC networks. IEEE Internet Things J, 2023, 10: 6336–6351

37 Gradshteyn I S, Ryzhik I M, Table of Integrals, Series, and Products, 6th ed. San Diego: Academic Press. 2000

38 Papazafeiropoulos A, Tran L N, Abdullah Z, et al. Achievable rate of a STAR-RIS assisted massive MIMO system under spatially-correlated channels. IEEE Trans Wireless Commun, 2023, 2: 1550–1564